JBC RESEARCH ARTICLE

The predicted stem-loop structure in the 3′-end of the human norovirus antigenomic sequence is required for its genomic RNA synthesis by its RdRp

Received for publication, May 17, 2021, and in revised form, September 13, 2021 Published, Papers in Press, September 23, 2021,
https://doi.org/10.1016/j.jbc.2021.101225

Takashi Shimoike*, Tsuyoshi Hayashi, Tomoichiro Oka, and Masamichi Muramatsu

From the Department of Virology II, National Institute of Infectious Diseases, Musashi-Murayama, Tokyo, Japan

Edited by Craig Cameron

The norovirus genome consists of a single positive-stranded RNA. The mechanism by which this single-stranded RNA genome is replicated is not well understood. To reveal the mechanism underlying the initiation of the norovirus genomic RNA synthesis by its RNA-dependent RNA polymerase (RdRp), we used an *in vitro* assay to detect the complementary RNA synthesis activity. Results showed that the purified recombinant RdRp was able to synthesize the complementary positive-sense RNA from a 100-nt template corresponding to the 3′-end of the viral antisense genome sequence, but that the RdRp could not synthesize the antisense genomic RNA from the template corresponding to the 5′-end of the positive-sense genome sequence. We also predicted that the 31 nt region at the 3′-end of the RNA antisense template forms a stem-loop structure. Deletion of this sequence resulted in the loss of complementary RNA synthesis by the RdRp, and connection of the 31 nt to the 3′-end of the inactive positive-sense RNA template resulted in the gain of complementary RNA synthesis by the RdRp. Similarly, an electrophoretic mobility shift assay further revealed that the RdRp bound to the antisense RNA specifically, but was dependent on the 31 nt at the 3′-end. Therefore, based on this observation and further deletion and mutation analyses, we concluded that the predicted stem-loop structure in the 31 nt end and the region close to the antisense viral genomic stem sequences are both important for initiating the positive-sense human norovirus genomic RNA synthesis by its RdRp.

Norovirus is a single-stranded positive-strand RNA virus that belongs to the *Caliciviridae* family. It is a major cause of acute gastroenteritis in humans. Its genome is approximately 7.5 knt long and typically encodes three open reading frames (ORFs). The 5′ untranslated region (UTR) (4–5 nt long) exists upstream of the ORF1. ORF1 encodes the viral nonstructural viral proteins (NS1-2, NS3 [NTPase], NS4 [3A-like protein], NS5 [VPg], NS6 [protease], and NS7 [RNA-dependent RNA polymerase; RdRp]), while ORF2 and ORF3 encode the major (VP1) and minor structural protein (VP2), respectively. A 3′ UTR (30–60 nt in length) exists downstream of the ORF3 and polyadenylated at its 3′ end halted (Fig. 1*A*) (1).

The viral RdRp is responsible for the replication/synthesis of the norovirus genomic RNA. RdRp first synthesizes antisense RNA using the genomic RNA as a template. It then uses these antisense RNAs to synthesize the progeny viral genomic RNAs. During replication, a subgenomic RNA encoding the ORF2 and 3 (3′ coterminal with the virus genome) is also synthesized in all members of the *Caliciviridae* (2).

Investigation into the RNA synthesis activity of the norovirus RdRp *in vitro* or cell-based systems has been reported (3–9). These papers proposed models of initiation of RNA synthesis by RdRp: when the template RNA has the polyA sequences at the 3′-end of the positive-sense genomic RNA, RdRp synthesizes the antisense RNA using the VPg protein primer (4, 6). When the RNA does not have the polyA sequences at the 3′-end of the antisense genomic RNA, the RdRp synthesizes the sense RNA without primers (3–5, 7–9). The importance of RNA stem-loop structures for recognition by the norovirus RdRp has also been reported (10).

To probe the initiation mechanism of the norovirus genomic RNA synthesis by its RdRp more deeply, we investigated here how the RdRp recognizes the antisense genomic RNA, which does not have the polyA sequences at the 3′-end, to initiate the synthesis of the complementary positive-sense genomic RNA. In this study, the viral genomic RNA template-specific RNA synthesis by the human norovirus (HuNV) RdRp was demonstrated for the first time in an *in vitro* assay. Results showed how the RdRp recognizes the antisense genomic RNA to initiate the synthesis of the complementary positive-sense genomic RNA.

Results

HuNV RdRp synthesizes the positive-sense RNA with the antisense viral genome template RNA carrying the 3′-end region

We used a nonradioactive labeling method to detect RNA synthesis by RdRp *in vitro* (a schematic of the procedures is shown in Fig. 1*A*). After the template RNA was incubated with the RdRp, RNA complementary to the template RNA was synthesized, forming a double-stranded RNA (dsRNA) with the template RNA. The dsRNA then remained after incubation with an S1 ribonuclease, to digest the single-stranded RNA into small nucleotides. Subsequently, the synthesis of the

* For correspondence: Takashi Shimoike, shimoike@nih.go.jp.

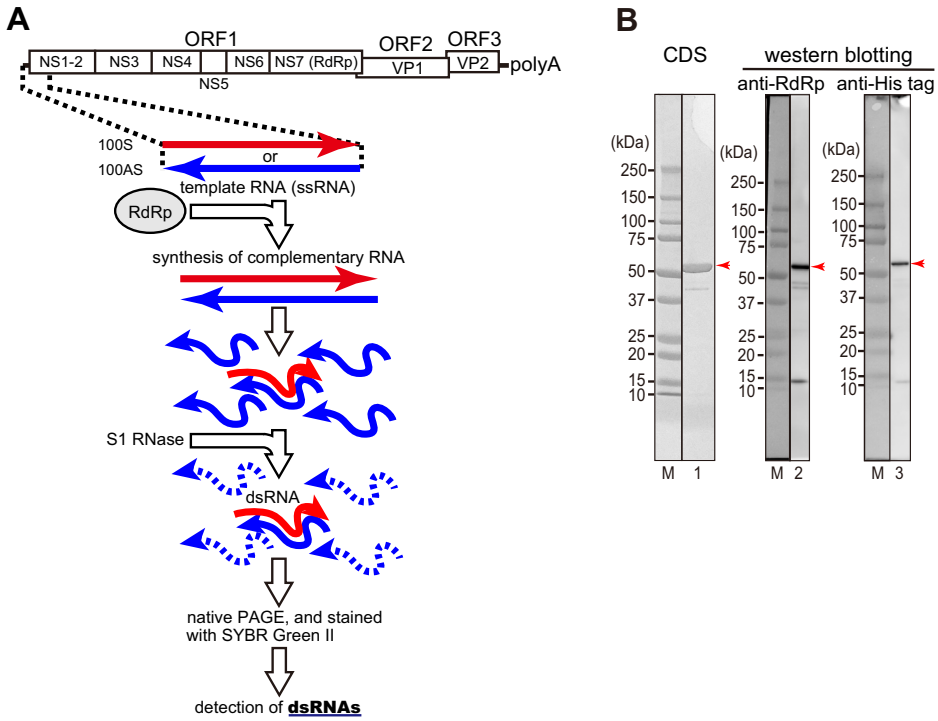

Figure 1. Schematic illustration of a nonradioactive labeling method to detect RNA synthesis by RdRp *in vitro* and characterization of the purified RdRp. *A*, as shown by *red* or *blue arrows*, respectively, the region of the RNA (positive sense or antisense (complementary) sequences of the 5′- or 3′-end 100 nt of the human norovirus genomic RNA) used as templates in this study is shown. Template single-stranded RNA (ssRNA) and norovirus RNA-dependent RNA polymerase (RdRp) were mixed and incubated to synthesize complementary RNA. The newly synthesized ssRNAs formed double-stranded RNA (dsRNA) with an excess of ssRNA templates. The ssRNAs in the reaction mixture were digested with S1 ribonuclease to visualize dsRNA only. RNA molecules before and after S1 ribonuclease treatment were separated by nondenaturing polyacrylamide gel electrophoresis (native PAGE) and stained with SYBR Green II. *B*, 31.7 nmol (lane 1) or 2.3 pmol (lanes 2 and 3) of the purified RdRp was performed using SDS-PAGE. After SDS-PAGE, the gel was visualized using Coomassie dye staining (CDS; lane 1) or detected with Western blotting using anti-RdRp antiserum (lane 2) or using anti-His-tag antibody (lane 3). M, molecular weight markers.

dsRNA is then used as an index that the RdRp synthesizes the complementary RNA in the following experiments.

The HuNV GII. P3 RdRp was tagged with six histidines at its N-terminus, expressed in *Escherichia coli* cells, purified, and analyzed by SDS-PAGE. The mobility of the major band was calculated as 57 kDa according to the molecular weight markers (lane 1 in Fig. 1*B*), and the band was detected by anti-RdRp and anti-His antibodies (lanes 2 and 3 in Fig. 1*B*, respectively). Finally, the purity of the RdRp was calculated as 96% (lane 1 in Fig. 1*B*).

The 5′ terminal nt 1 to 100 of viral genomic RNA of the HuNV GII. P3 strain (100S [sense]) or its complementary sequence (100AS [antisense]) was then used as template RNAs (see Fig. 1*A*). All the template RNAs used here carry GGG and CCC sequences at their 5′- and 3′-ends, respectively, to efficiently synthesize template RNAs *in vitro* and form stable dsRNAs. When increasing amounts of RdRp were incubated with 100S RNA, almost no RNA was synthesized (lanes 4–7 on the upper column in Fig. 2*A*). However, when increasing amounts of RdRp were incubated with 100AS RNA, dsRNA was synthesized in increasing amounts (lanes 8–11 in the upper column in Fig. 2*A*). To confirm that these synthesized RNAs were dsRNAs, the RNAs were treated with S1 ribonucleases. The amounts of the synthesized dsRNA were then increased according to the amounts of the RdRp (lanes 8–11 in the lower column in Fig. 2*A* and the graph in Fig. 2*B*). The efficient activity of S1 ribonucleases was confirmed by the fact that the marker ssRNAs (100S and 100AS) were digested well, but the dsRNA (ds100) markers were resisted with S1 ribonuclease treatment (lanes 1, 2, and 3 on the lower column in Fig. 2*A*, respectively). These results therefore indicate that the RdRp specifically recognizes the 3′-end of the antisense viral genome RNA and indicate also that this region is important to initiate the synthesis of the positive-strand RNA by the RdRp.

The predicted stem-loop structure and the region close to the stem are required for initiating the synthesis of the positive-sense RNA by the RdRp

We examined the secondary structure in the 3′-end regions of the antisense genomic RNA of HuNV GII.P3 strain. We found that nt 74 to 87 (located at the 3′-terminus) in the 100AS RNA forms a predicted stem-loop structure (see Experimental procedures and Fig. 3*A*). The sequence of nt 74 to 100 was highly conserved among the norovirus genogroups I, II, IV, and VII (Fig. 3*B*). To determine whether this stem-loop (nt 74–87) was important for initiating RNA synthesis by the RdRp, a deletion mutant of 100AS RNA that lacks the 31 nt (nt 70–100) at the 3′-terminus of the 100AS RNA was constructed (designated as Δ31AS RNA, Fig. 4*A*). Its complementary template RNA was also constructed as a control (designated as Δ31S RNA). When Δ31AS RNA and Δ31S RNA were used as template RNAs, the RdRp did not synthesize the

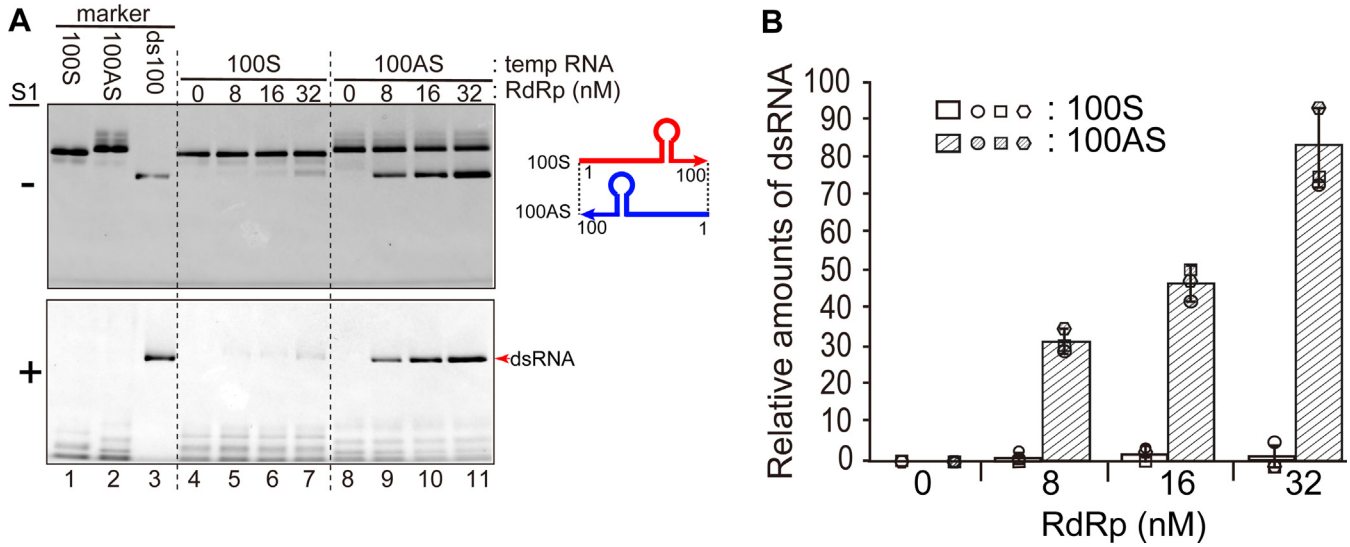

Figure 2. The RdRp synthesizes the complementary RNA from 100AS RNA template. *A, in vitro* synthesized RNAs separated in native PAGE. The template ssRNAs [100S RNA (lane 1), 100AS RNA (lane 2)], and ds100 RNA (lane 3) were used as size markers. Five pmol of each template RNA, *i.e.*, 100S (100 nM, lanes 4–7) or 100AS (100 nM, lanes 8–11), and the purified HuNV RdRp (0–32 μM) were mixed. Half of the total volume of samples was mixed with 6× gel-loading buffer and loaded on native PAGE (the *upper column*). S1 ribonuclease was added to the remaining half of the samples, and the samples were incubated and loaded on native PAGE (the *lower column*). The dsRNA products separated in native PAGE before and after S1 ribonuclease treatment are shown in the *upper* and *lower columns*, respectively. *Red arrow* indicates newly synthesized RNA products, which had formed dsRNAs with an excess of template RNA and identically migrated to dsRNA markers (lanes 4–11). *B*, the relative amounts of the newly synthesized dsRNA products (the transcriptional activity) were analyzed using ImageJ v.2.1.0/1.53c computer software and shown as the graph. The amounts shown were the averages of three experiments. The standard deviations are also shown in the graph. Each result of the three independent experiments is also shown by the three kinds of shapes (*circles*, *rectangles*, and *hexagons*).

complementary RNA from either template RNAs (lanes 11 and 13 at the upper column in Fig. 4*A*). To remove the single-stranded template RNA to confirm the synthesis of the dsRNA, the reaction products shown on the upper column in Figure 4*A* were treated with S1 ribonucleases. Absent or faint RNAs were detected (lanes 11 and 13 in the lower column in Fig. 4*A*, respectively). These results therefore indicate that nt 70 to 100 of 100AS RNA containing the predicted stem-loop structure is necessary for initiating the complementary positive-strand genomic RNA synthesis by the RdRp.

To confirm that the 31 nt RNA, carrying the nt 70 to 100 of 100AS RNA (31AS RNA, shown in Fig. S1), was sufficient for RNA synthesis by the RdRp, two chimeric RNA templates were further prepared: (i) the 5′-end of 31AS RNA was connected to the 3′-end of the Δ31S RNA (designated as add31AS-S), and (ii) the 3′-end of 31S RNA was connected to the 5′-end of the Δ31AS RNA (designated as add31S-AS and complementary to add31AS-S RNA, Fig. S1). The RdRp also synthesized dsRNA with add31AS-S RNA as the template, but a few amounts of dsRNA were detected when the complementary add31S-AS RNA was used as a template (lanes 11 and 13, respectively, in Fig. 4*B*). These results therefore confirmed the importance of the 31 nt region at the 3′-end of antisense genomic RNA for the RdRp activity.

Similarly, to narrow down the regions in nt 70 to 100 of the 100AS RNA responsible for initiating RNA synthesis by the RdRp, the following deletion mutants were constructed: Δ6AS, Δ9AS, and Δ12AS RNA, in which nt 95 to 100, nt 92 to 100, or nt 89 to 100 were deleted, respectively (Fig. 4*C*). The result showed that the RdRp synthesized dsRNAs derived from Δ6AS and Δ9AS, respectively, to the same extent as that of the 100AS RNA, whereas the synthesis of dsRNA from the Δ12AS RNA template was much less efficient (Fig. 4*C*), indicating that the nt 90 to 100 is not important for initiating dsRNA synthesis.

To know the importance of the stem-loop region (nt 74–87), three kinds of mutant template RNAs were also constructed: (i) Δsl (stem-loop) AS RNA, in which the stem-loop region (nt 74–87) was deleted (Fig. 4*D*); (ii) sw (switch) AS RNA, in which the stem regions, nt 75 to 78 and nt 83 to 86, were switched together to preserve the stem structure (Fig. 4*E*); and (iii) lp (loop) AS RNA, in which nt 79 to 82 (GUUA) at the top loop of the stem loop in the 100AS RNA was changed to the complementary sequence (CAAU) (Fig. 4*F*). When the ΔslAS and swAS RNAs were used as templates for RdRp, small amount of the dsRNAs was synthesized (lane 13 in Fig. 4, *D* and *E*, respectively). Alternatively, dsRNA was synthesized as well with lpAS RNA (lane 13 in Fig. 4*F*). These results, therefore, also indicate that the stem-loop region is important, and the stem region (nt 74–78 and nt 83–87) is more important than the top-loop region (nt 79–82) (see Fig. 3). All these results of the activities of 100S, 100AS, and its mutated template RNAs are summarized in Fig. S2.

Interaction of the 3′-end of 100 nt antigenomic RNA with the RdRp

The direct interaction of 100AS RNA with the RdRp was examined by the electrophoretic mobility shift assay (EMSA) technique using RNAs labeled with ^{32}Phosphate at the 5′-end. When 100AS RNA was incubated with the RdRp, the amount of the RNA-RdRp complex increased as the amount of the RdRp increased (lanes 1–4 in Fig. 5*A*). However, when Δ31AS RNA lacking in the 31 nt of the 3′-end of the 100AS RNA was incubated

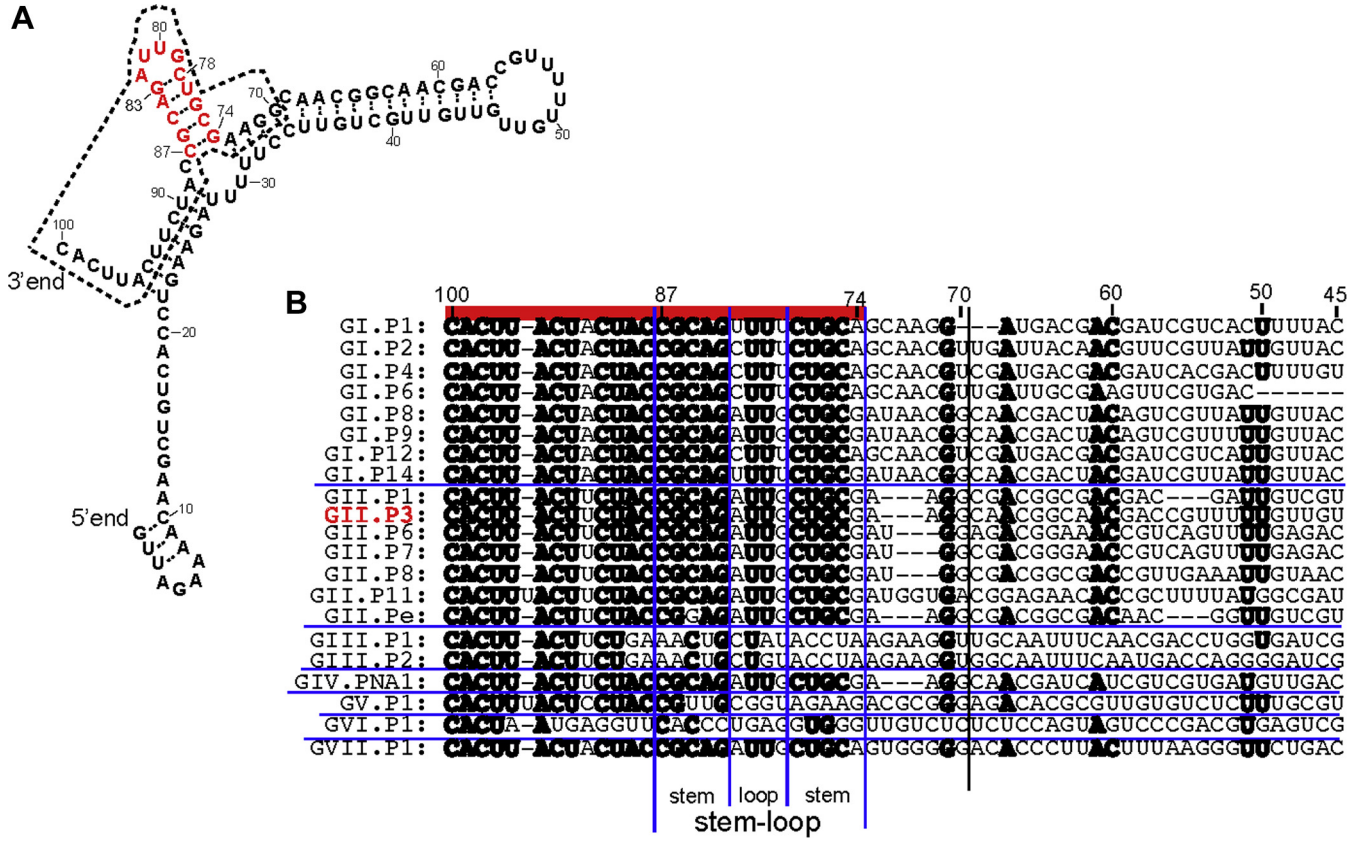

Figure 3. The predicted secondary structure of 100AS HuNV RNA. *A*, the 100AS RNA secondary structure was predicted using the computer software (23). The region of 31AS RNA (nt 70–100 of the U201 strain) is surrounded by a *dotted line*, and *red characters* indicate nt 74 to 87, which form the predicted stem-loop structure. *B*, alignments of 21 kinds of norovirus genotypes at the 3′-end regions of the antisense genome sequences (nt 100–45 of 100AS RNA of the GII. P3 U201 strain and its corresponding regions of other genotypes) are shown. The nucleotides with more than 71% identity (the same nucleotide in more than 15 of the total 21 genotypes) are indicated in *bold*. RdRp-coding genes are used to classify the genotypes (24). *Horizontal blue lines* separate genogroups. *Red line* on the *top* indicates highly conserved regions (nt 100–74 regions of the GII.P3 U201 strain). The 31AS RNA region is indicated by separating with a *vertical black line* between nt 69 and 70. Four *vertical blue lines* show the separation in the stem and loop regions in the stem-loop regions. The GII. P3 U201 strain that was used in this paper is shown in *red characters*.

with increasing amounts of the RdRp, Δ31AS RNA formed a complex with the RdRp much less efficiently than 100AS RNA even at the highest concentration (lanes 5–8 in Fig. 5*A*). These results indicate that the 31 nt is recognized by the RdRp with high affinity and implies that this recognition is required for the initiation of genome positive-strand RNA synthesis.

To confirm that this interaction was specific, two nonlabeled RNAs, 100AS RNA and Δ31AS RNA, were used as competitors in EMSA (Fig. 5*B*). When the ^{32}P-labeled 100AS RNA was incubated with increasing amounts of the same nonlabeled 100AS RNA, the amount of the labeled RNA-RdRp complex decreased in correspondence with the increase in nonlabeled 100AS RNA. The amount of the shifted RNA-RdRp complex decreased to 13.5% (lanes 1–5 in Fig. 5*B*). In contrast, when ^{32}P-labeled 100AS RNA was mixed with increasing amounts of nonlabeled Δ31AS RNA lacking in nt 70 to 100 at the 3′-end of 100AS RNA, the ^{32}P-labeled 100AS RNA-RdRp complex competed with nonlabeled Δ31AS RNA, but the efficiency of competition with nonlabeled Δ31AS RNA (decreased to 35.8%) was lower than that with the nonlabeled 100AS RNA (decreased to 13.5%). These results thus indicate that the 100AS RNA and the RdRp interact specifically and imply that the 31 nt RNA (31AS RNA) is required for this interaction.

Similarly, since the 31AS RNA (the nt 70–100 of 100AS RNA, see Fig. S1) was important for initiating genomic RNA synthesis by the RdRp as demonstrated above (lanes 13 and 11 in Fig. 4, *A* and *B*, respectively); EMSA was used to examine the interaction of the 31AS RNA with the RdRp. The ^{32}P-labeled 31AS RNA was incubated with increasing amounts of the RdRp. However, no 31AS RNA-RdRp complex was detected even at the highest concentration (600 pmol) of the RdRp (lanes 9–12 and the graph in Fig. 5*A*). Also, when the nonlabeled 31AS RNA was used as a competitor for the complex of 100AS RNA and RdRp, the competition was less efficient than when using the nonlabeled 100AS RNA as a competitor (decreased to 47.3% *versus* 13.5%, lanes 11–15 *versus* lanes 1–5 and the graph in Fig. 5*B*). It is possible that the 31AS RNA was too short to form the stable complex with the RdRp efficiently. Therefore, to determine whether the 31AS RNA region interacted with the RdRp, the interaction of the RdRp with add31AS-S RNA (the structure formed by connecting the 5′-end of 31AS RNA to the 3′-end of Δ31S RNA (see Fig. S1)) was examined using EMSA. When the ^{32}P-labeled add31AS-S RNA was incubated with the RdRp, the amount of the RNA-RdRp complex increased in correspondence with the amounts of the RdRp (lanes 5–8 and the graph

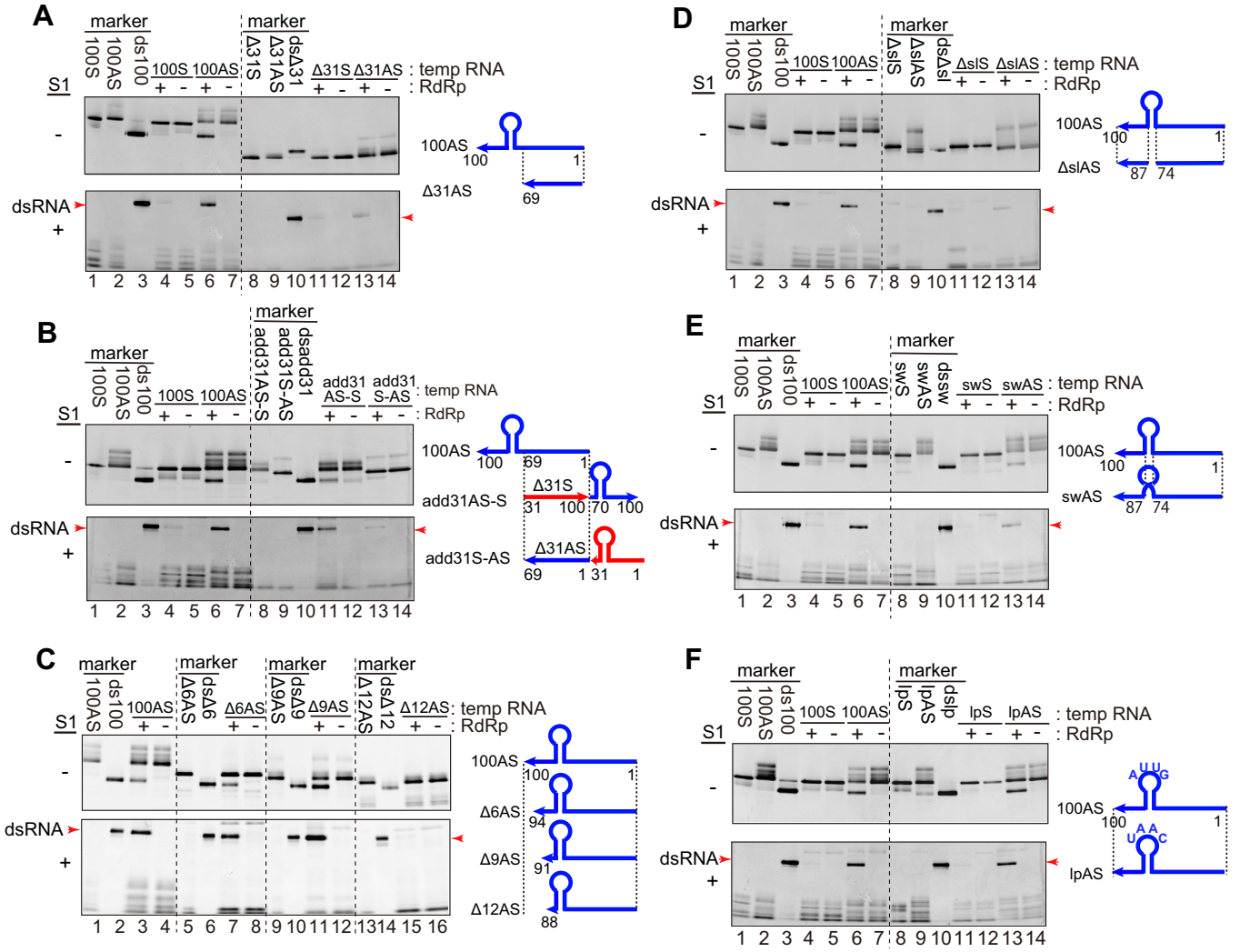

Figure 4. The RNA synthesis with mutated template RNAs by the HuNV RdRp. Five pmol of each template RNA (final concentration, 100 nM) and 0.8 pmol HuNV RdRp (final concentration, 16 μM) were mixed. After incubation, half of the samples were loaded on native PAGE (the *upper column*). The other half of the samples were treated with S1 ribonucleases and loaded on native PAGE (the *lower column*). The results using templates, Δ31S and Δ31AS RNAs (*A*); add31AS-S and add31S-AS RNAs (*B*); Δ6AS, Δ9AS, and Δ12AS RNAs (*C*); ΔslS and ΔslAS RNAs (*D*); swS and swAS RNAs (*E*); and lpS and lpAS RNAs (*F*), were shown, respectively. The template ssRNA (lanes 1, 2, 8, and 9) and dsRNA (lanes 3 and 10) were used as size markers in *A*, *B*, and *D–F*. The template ssRNA (lanes 1, 5, 9, and 13) and dsRNA (lanes 2, 6, 10, and 14) were used as size markers in *C*. The positions of each dsRNA are indicated with *red arrows* in the *lower columns*. All results are representative of at least triplicate experiments. The schematic structures of the 100S, 100AS, and its mutated template RNAs are shown on the *right side* of each figure.

in Fig. 5*C*). However, the Δ31S RNA itself (nt 31–100 of the positive-sense RNA) did not have an activity to synthesize the complementary RNA by the RdRp (lane 11 in Fig. 4*A*). It also did not form a complex with the RdRp (lanes 9–12 and the graph in Fig. 5*C*). Finally, these results show that 31AS RNA is required for interacting with the RdRp and required for initiating RNA synthesis as well.

Inhibitory effects of nucleoside analogs on the RNA synthesis by the HuNV RdRp

We examined whether our *in vitro* assay detected RdRp inhibitory effects by compounds. We tested 2′-C-methylcytidine (2′CM) and its ribonucleotide triphosphate form, 2′-C-methylcytidine triphosphate (2′CM-CTP), as known inhibitors of the HuNV RdRp. When increasing concentrations of 2′CM were added to the reaction mixture, no inhibitory effect on the RNA synthesis was observed (lanes 3–7 at the lower column and the graph in Fig. S3). However, when increasing concentrations of the converted form, 2′CM-CTP, were added to the reaction mixture, the amounts of synthesized dsRNA were decreased from 100% to 0.5% (lanes 8–12 and the graph in Fig. S3). Our result was also consistent with previous studies and reasonable because it is known that 2′CM has an inhibitory effect after it is converted to the ribonucleotide triphosphate form, 2′-C-methylcytidine triphosphate (2′CM-CTP) by cellular kinases (11, 12). The IC_{50} (half of the maximal inhibitory concentration) of 2′CM-CTP was calculated as 57 ± 20 μM.

Discussion

We determined here that the HuNV RdRp initiates the template-specific initiation of RNA synthesis, and that the RdRp interacts with the 3′-end region of the antisense genomic RNA.

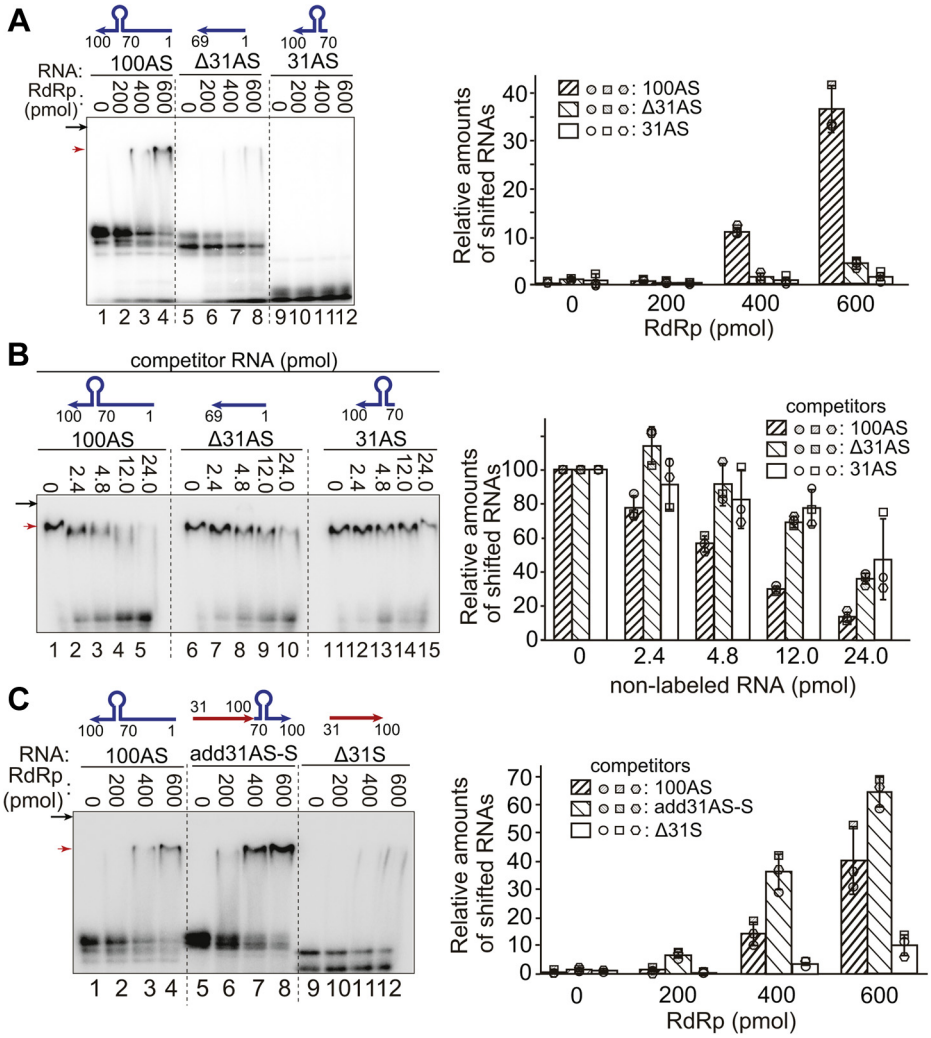

Figure 5. Interaction of the template 100AS RNA and its mutated RNAs with RdRp by EMSA. *A*, the ^{32}P-labeled 5′-end-labeled RNAs (100AS; lanes 1–4, Δ31AS; lanes 5–8, or 31AS; lanes 9–12, 1 pmol each) and the RdRp (0–600 pmol) were incubated. *B*, the ^{32}P-labeled 5′-end-labeled 100AS RNA (0.2 pmol), the indicated number of non-labeled competitor RNAs; 100AS (lanes 1–5), Δ31AS (lanes 6–10), or 31AS RNA (lanes 11–15) and the RdRp (600 pmol) were incubated. *C*, the ^{32}P-labeled 5′-end-labeled RNAs (1 pmol); 100AS (lanes 1–4), add31AS-S (lanes 5–8), or Δ31AS (lanes 9–12) RNAs and the RdRp (0–600 pmol) were incubated. After incubation, EMSA was used to examine all the samples. The relative amounts of RNAs that were complexed with the RdRp (the shifted RNAs) were analyzed using ImageJ v. 2.1.0/1.53c computer software and shown as the graph. The amounts were the averages of three times experiments. The standard deviations are shown in the graph. Each result of the three independent experiments is also shown by the three kinds of shapes (*circles*, *rectangles*, and *hexagons*). *Black arrows* indicate the position of the bottom of wells. *Red arrows* indicate the RNA-RdRp complex. The schematic structures of labeled RNAs (*A* and *C*) or nonlabeled competitor RNA (*B*) are shown on each RNA.

First, we demonstrated that the HuNV RdRp synthesized complementary (positive-strand genomic) RNA from the 100 nt of the 3′-end region of the antisense genomic template RNA (100AS RNA), but did not synthesize the antisense RNA from the 100 nt of the 5′-end region of the genomic template RNA (100S RNA) (Fig. 2*A*). Similarly, the introduction of deletions and mutations in the 31 nt region revealed that the predicted stem-loop region and the region close to the stem sequences are required as a template for RNA synthesis by the RdRp. There are reports on the activity of the HuNV RdRp *in vitro*, and the template RNAs used in these reports are those corresponding to partial 3′-terminal genomic or sense/antisense subgenomic sequences of HuNV (3, 4, 7, 9) or a nonviral template (5, 7, 8). The HuNV RdRp has the activity to synthesize the complementary RNAs using any sequences of the template RNAs used in these reports. In contrast, we demonstrated the genomic sequence specificity of template RNA. The genome specificity would come from the concentrations of the RdRp in the reaction mixture; the concentration of the RdRp used in these reports was about 30 to 200 times higher than that used in this study.

Second, we also demonstrated the interaction of HuNV RdRp with antisense genomic RNA by using EMSA. Our results showed that the RdRp forms a complex with 100AS RNA, and the specific interaction was shown by competition with the same nonlabeled 100AS RNA. The deletion of nt 70 to 100 in 100AS (Δ31AS RNA) also caused a loss in the interaction with the RdRp in EMSA, and the competition with Δ31AS RNA was less efficient than that with 100AS for the 100AS RNA-RdRp binding. These results indicate that the nt 70 to 100 (31 nt) was required for the interaction with the RdRp (Fig. 5, *A* and *B*). The add31AS-S RNA, which is composed of the

connection between the 5′-end of 31AS RNA and the 3′-end of Δ31S RNA (shown in Fig. S1), formed the complex with the RdRp by EMSA (Fig. 5*C*). These results also show that the nt 70 to 100 in 100AS RNA (31AS RNA) is required for interaction with the RdRp. As shown in Figure 4*B*, the add31AS-S RNA was active as a template for the RdRp. Finally, these results imply that the 3′-end (the nt 70–100) of the antisense genomic RNA is required for recognition and initiation by the RdRp for synthesis of positive-sense genomic RNA.

As shown in Figure 3, the regions containing the predicted stem-loop structure are important for recognizing and initiating the synthesis of the positive-sense genomic RNA by the norovirus RdRp. Simmonds *et al.* have reported predicted secondary structures at three locations: the 5′-end, 3′-end, and the upstream of the subgenomic RNA in the whole HuNV and murine norovirus (MNV) genomic and antigenomic RNAs. They also showed that all of these regions are important for MNV genome replication (10). Additionally, the upstream subgenomic region was shown as a promoter of the antisense subgenomic RNA (10, 13, 14). Likewise, the importance of the stem-loop structure located close to the end of the genomic or antisense genomic RNA in the synthesis of viral genomic or antigenomic RNA by viral RdRp has also been reported in other nonsegmented single-stranded positive-sense RNA viruses (*e.g.*, dengue virus [DENV], hepatitis C virus [HCV], and classical swine fever virus [CSFV]) (15–17).

The nt 74 to 100 region of GI, GII, GIV, and GVII noroviruses antisense genomic RNA is highly conserved among genogroups, although the GIII, GV, and GVI genogroups are different from this "conserved sequence" (Fig. 3*B*). This result also indicates that this mechanism of initiation of viral genomic RNA synthesis by the RdRp is common among many genogroups, especially the GI, GII, GIV, and GVII genogroups, which infect humans and canines, respectively.

As we reported here, the 31 nt RNA located at the 3′-end region of the antisense HuNV genomic RNA, which contains the predicted stem-loop structure, is required to bind to the RdRp and to initiate the RNA synthesis by the RdRp. In GI, GII, GIV, and GVII noroviruses, the nt 74 to 100 regions corresponding to the 3′-end regions of the antisense subgenomic RNA are also highly conserved and homologous to those of the antisense genomic RNA (Fig. S4 and Fig. 3*B*). This implies that nt 74 to 100 of the antisense subgenomic RNA also forms the stem-loop structure the same as the antisense genomic RNA; also, the mechanism of the synthesis of the subgenomic RNA by the RdRp is probably the same.

The RdRp also interacts with other stem-loop RNA regions (promoter for synthesizing the subgenomic RNA), the complementary sequences of which are located upstream of the antisense genomic RNA, and initiates the RNA synthesis (10, 13, 14).

These results imply that the norovirus RdRp binds to at least three regions of stem-loop structures in the antisense genomic RNA (Fig. S5); as we reported here, the one (indicated as 1 in Fig. S5) is located close to the 3′-end of the antisense genomic RNA to synthesize the genomic RNA. The second one (indicated as 2 in Fig. S5) is located at the 3′-end of the antisense subgenomic RNA. The third one (indicated as 3 in Fig. S5) is the promoter sequence synthesizing the subgenomic RNA from the antisense genomic RNA (13, 14). The sequences and structures have a high similarity between regions 1 and 2 (Fig. S4). Therefore, it is important to know how the RdRp distinguishes these three regions (1, 2, and 3) to bind and initiate RNA synthesis in the next stage. We proposed one model for the RdRp recognition of region 2 and region 3: the RdRp binds to region 3 (promoter) in the antisense genomic RNA preferentially, but once region 2 becomes the 3′-end after the antisense subgenomic RNA is synthesized, the RdRp binds to region 2 preferentially. Host cell factors, other viral proteins, and/or the conformational changes after RdRp binds to these regions might control which regions the RdRp binds preferentially to initiate the syntheses of genomic or subgenomic RNAs.

The nucleoside analog inhibitor of RdRp, 2′-C-methylcytidine (2′CM), was initially an HCV inhibitor (12). It works as a chain terminator and competes with CTP during the synthesis of genome RNA by viral RdRp. We also showed that 2′CM-CTP inhibited the synthesis of the viral genomic RNA by the HuNV RdRp (Fig. S3). The IC_{50} was 57 ± 20 μM. This inhibitory efficiency on HuNV was similar to that reported by Jin *et al.* (7) (IC_{50} is 33.6 ± 5.8 μM). Similarly, several antiviral drugs have been developed so far, and most of them are direct-acting antivirals (DAAs) that selectively target viral components (*e.g.*, RdRp, helicase, or protease) without affecting cellular function, thus minimizing side effects (18, 19). Our *in vitro* RdRp assay system will therefore be a valuable tool to screen seed compounds for developing DAAs against HuNV RdRp.

Conclusively, we identified the regions in the antigenomic HuNV RNA that are required for the interaction and initiation of the genomic RNA synthesis by its RdRp *in vitro*.

Experimental procedures

Plasmid architecture

The plasmid for expressing the RdRp protein coding for the cDNA (nt 3581–5113) of the human norovirus GII. P3_GII.3 U201 strain (accession no. AB039782) (20) was amplified by PCR using the specific primers containing the NdeI restriction sites at the 5′-end, the stop codon (TAA), and the XbaI restriction site at the 3′-end (shown in the table in Supporting information). Thereafter, it was cloned into the NdeI-XhoI site of the pET28b vector (Merck Millipore) (designated pET28b-RdRp).

All plasmids for the template RNAs were prepared by PCR using nt 1 to 100 cDNA corresponding to the 5′-terminal of the genomic RNA of the human norovirus GII.P3_GII.3 U201 strain (corresponding to the positive strand) or its complementary sequence (corresponding to the antisense strand), specific primers containing the XbaI restriction site-T7 promoter sequences-three Gs (GGG) at the 5′-end, or three Cs (CCC) at the BsaI-EcoRI sites at the 3′-end (shown in the table in Supporting information), and Ex Taq DNA polymerase (Takara). The amplified DNA fragments were then cloned into the same restriction sites of pUC19 vector (Takara). When the

plasmids, pUCadd31AS-S and pUCadd31S-AS, were prepared, pUCΔ31S or pUCΔ31AS was used as the DNA template for PCR. Similarly, all the plasmids for the template RNA were designed to carry GGG and CCC sequences at the 5′- and 3′-ends, respectively. This plasmid was then used to synthesize template RNAs efficiently by T7 polymerase and to form the stable dsRNAs.

Preparation of the HuNV RNA-dependent RNA polymerase (RdRp)

E. coli cells, ArcticExpress (DE3) (Agilent Technologies, Inc) carrying the pET28b-RdRp were cultured in 1 l of Luria Broth Base medium (Invitrogen) at 30 °C until the turbidity at the optical density $(OD)_{590}$ was approximately 0.6 (for up to 3 h) and then placed in ice-cold water for 20 min. Next, isopropyl β-D-1-thiogalactopyranoside (final concentration, 1 mM; Wako) was added, and the cells were cultured for an additional 24 h at 13 °C. To purify RdRp (His-RdRp) containing a His tag at the N-terminus, the culture was then centrifuged at 4400*g* on a JLA-10.500 rotor (Beckman Coulter) for 5 min. Afterward, 20 ml of buffer (50-mM Tris-HCl (pH 7.5), 150-mM NaCl, and 5-mM β-mercaptoethanol) was added to the bacterial pellets, and the pellets were suspended in the buffer and sonicated by five rounds of a 30 s on ¾-in. chip at an intensity level of 5 with subsequent cooling in iced water (Astrason Ultrasonic Processor XL-2020; Misonix, Inc). The sample was then centrifuged at 22,700*g* on a JA-20 rotor (Beckman Coulter) for 15 min, after which the supernatants were loaded onto a 2.5-ml buffer-equilibrated Ni-NTA column (Qiagen). After washing the column first with 200-ml buffer, and then with 15-ml His-A buffer (50-mM Tris-HCl (pH 7.5), 150-mM NaCl, 5-mM β-mercaptoethanol, 10-mM imidazole), His-RdRp was eluted with 10-ml elution buffer (50-mM Tris-HCl (pH 7.5), 150-mM NaCl, 5-mM β-mercaptoethanol , 200-mM imidazole). The His-RdRp was subsequently purified further with a buffer-equilibrated gel filtration column (HiLoad 16/60 Superdex 200; GE Healthcare).

Detection of RdRp with Coomassie dye staining and Western blotting

Here, 31.7 nmol (lane 1) or 2.3 pmol (lanes 2 and 3) of the purified RdRp was analyzed by SDS-PAGE. After SDS-PAGE, lane 1, the gel stained with Coomassie dye, GelCode Blue Stein Reagent (Thermo Fisher Scientific) was used to visualize the purified RdRp. Similarly, in lanes 2 and 3, proteins on the gel were transferred to the polyvinylidene fluoride (PVDF) membrane with iBlot Gel Transfer Stacks PVDF, regular (#IB401001, Thermo Fisher Scientific). The two PVDF membranes were then blocked with PVDF-blocking reagent, Can-Get Signal (TOYOBO) for 1 h at room temperature (RT). One PVDF membrane (lane 2) was incubated with 1/1000 diluted anti-RdRp antiserum (anti-Guinea Pig, polyclonal against RdRp of GII.P3U201 strain, Eve bioscience). The other PVDF membrane (lane 3) was incubated with 1/1000 diluted anti-6X His-tag antibody (anti-6X His-tag antibody #ab9108; Abcam) in a Can Get Signal Immunoreaction Enhancer Solution 1 (#NKB–201; TOYOBO) at 37 °C for 1 h, respectively. The two PVDF membranes were washed with TBS Tween20 (10-mM Tris-HCl [pH 7.5], 150-mM NaCl, 0.05% Tween20) for 15 min three times, after which the PVDF membrane incubated with anti-RdRp serum or the other PVDF membrane incubated with anti-His tag antibody was then incubated with antibodies: 1/30,000 diluted Peroxidase-AffiniPure Donkey Anti-Guinea Pig IgG (H + L) (#706-035-148; Jackson ImmunoResearch Laboratories), or 1/30,000 diluted Goat anti-Rabbit IgG (H + L) HRP-conjugated (#1706515; Bio Rad) in a Can Get Signal Immunoreaction Enhancer Solution 2 (#NKB–301; TOYOBO) at RT for 1 h, respectively. After this step, the two PVDF membranes were washed with TBS Tween20 for 15 min three times again and then detected with a Super Signal WestFemto Maximum Sensitivity Substrate (#34096; Thermo Fisher Scientific). The RdRp was detected using the LAS-3000 imaging analyzer (Fujifilm). The purity of RdRp was subsequently calculated using ImageJ v.2.1.0.

Preparation of template RNAs

Fifty micrograms of each plasmid was digested using BsaI (New England Biolabs) to exclude the nonviral sequences at the 3′-end. RNA was then synthesized from a template of the linearized DNA using T7 polymerase and purified with a gel filtration column (HiLoad 16/60 Superdex 75, or 200) (the purity of RNAs; at least 90%) as described by Mckenna *et al.* (21) and Shimoike *et al.* (22).

The 5′-end ^{32}P-labeled template RNAs were prepared as follows: the calf intestinal alkaline phosphatase (Takara) was used to dephosphorylate the 5′-end of the purified template RNAs. Subsequently, the ^{32}Phosphate was bound to the 5′-end of the dephosphorylated template RNA by the T4 polynucleotide kinase (Takara), followed by phenol/chloroform, and precipitated by ethanol. The unreacted γ-32P-ATP in the RNA was then removed using Sephadex G-50 fine resin (GE Healthcare). The ^{32}P-labeling efficiencies of RNAs were found to be 49% to 51%.

Assay for RNA synthesis by RdRp

A 5-pmol template RNA (final concentration, 100 nM) and 0.8-pmol HuNV RdRp (final concentration, 16 nM) were mixed with the reaction buffer (20-mM Tris-HCl [pH 7.4], 5-mM DL-Dithiothreitol, 2-mM NTPs (ATP, UTP, GTP, CTP; Sigma Aldrich), 2-mM $MnCl_2$, 0.8-U/μl ribonuclease inhibitor (Toyobo)) and incubated at 30 °C. The mixture was divided into two portions (20 μl each) 30 min after incubation. To one portion, 4 μl of 6× gel-loading buffer (10% glycerol, 0.02% BPB, 0.01% xylene cyanol in TBE buffer [89-mM Tris, 89-mM borate, 2-mM EDTA]) was added, and nondenaturing polyacrylamide gel electrophoresis (native PAGE) with the running buffer (25-mM Tris, 192-mM glycine, pH 8.3) was performed at a constant voltage of 300 V for 25 min (5%–20% polyacrylamide gel [ePAGEL, ATTO]). To the other portion, 7 μl of ten times diluted S1 nuclease (89 U/μl; Promega) and 3 μl of S1 ribonuclease buffer were added and incubated for 30 min at 30 °C to degrade the ssRNA and detect double-stranded RNA

(dsRNA) comprising the template RNA and the newly synthesized complementary strands. After this step, the 6× gel-loading buffer was then added, and the native PAGE was performed as described above. After native PAGE, the gel was then stained with SYBR Green II (LONZA) and detected using a LAS-3000 imaging analyzer (Fuji Film).

Prediction of the RNA secondary structure and alignments of NV antisense genome sequences

The nucleotide secondary structure of the 100AS RNA (nt 1–100, GII.P3 U201 strain) was predicted using the Genetyx-Mac software v.19.0.3 (Genetyx Corporation) by "RNA secondary structure prediction" (23) using default settings. The alignments of the 3′-end 100 nt regions of the norovirus antisense genomic or antisense subgenomic RNA sequences were then calculated using the Genetyx-Mac software v.19.0.3 (Genetyx Corporation) from "multiple alignments" with default settings. The nt 100 to 45 regions of the antisense genomic and antisense subgenomic RNAs are shown, respectively. Similarly, the accession numbers of these 21 sequences are as follows: GI. P1: M87661; GI. P2: L07418; GI. P4: AB042808; GI. P6: AF093797; GI. P8: KJ196298; GI. P9: KF586507; GI. P12: AB039774; GI. 14: AB187514; GII. P1: U07611; GII. P3: AB039782 (used in this paper); GII. P6: AB039778; GII. P7: AB039777; GII. P8: AB039780; GII. P11: AB126320; GII. Pe: AB434770; GIII. P1: AJ011099; GIII. P2: AF097917; GIV. PNA1: KX907728; GV. P1: AY228235 (MNV-1); GVI. P1: FJ875027; and GVII. P1: FJ692500.

Electrophoretic mobility shift assay (EMSA)

The ^{32}P-labeled 5′-end-labeled RNA (1 pmol) and the RdRp (200, 400, 600 pmol) were incubated in the reaction buffer (50-mM Tris-HCl pH 7.4, 1.7% glycerol, 5-mM β-mercaptoethanol, and 0.5 μg/μl of yeast RNA [Thermo Fisher Scientific]) at 30 °C for 10 min (total volume, 20 μl). A 4 μl of 6× gel-loading buffer was then added to the reaction mixture. The RNA and RdRp complex was separated with native PAGE at a constant voltage of 60 V for 90 min at 4 °C in the 1/2 × running buffer (12.5-mM Tris, 86-mM glycine, pH 8.3) after the gel was prerun at a constant voltage of 60 V for 30 min at 4 °C and analyzed by Typhoon FLA 7000 image analyzer (GE Healthcare). In the case of the competition assay, the procedures are the same as above except that the nonlabeled RNA (0, 2.4, 4.8, 12.0, or 24.0 pmol) was incubated with ^{32}P-labeled 100AS RNA (0.2 pmol) and the RdRp (600 pmol), respectively.

Assay for inhibitory effects of the nucleoside analog on RNA synthesis

2′-C-methylcytidine (2′CM, Merck) and 2′-C-methylcytidine triphosphate triethylammonium salts (2′CM-CTP, Carbosynth Limited) were added (final concentration of 0, 1, 10, 100, or 500 μM) to the reaction mixture that is the same content described in the Assay for RNA synthesis by RdRp except for the concentration of NTPs (800 μM each) and incubated at 30 °C for 60 min, after which the dsRNA signal was detected as described above. The chemical compound concentrations resulting in a 50% reduction in dsRNA drug-free control production were determined based on the dose–response curve and defined as the mean 50% inhibitory concentration (IC_{50}) values of the RdRp activity.

Data availability

All data are contained within the manuscript

Supporting information—This article contains supporting information (10, 13, 14, 24).

Acknowledgments—We are grateful to Dr Yoshiaki Okada and all the members of our department for their assistance. We thank Prof. Joseph D. Puglisi for editing the manuscript. We also thank Dr Kazuhiko Katayama for the RNA of the norovirus GII.P3_GII.3 U201 strain.

Author contributions—T. S. conceptualization; T. S. data curation; T. S. formal analysis; T. S. and M. M. funding acquisition; T. S. investigation; T. S. methodology; T. S. project administration; T. S. resources; T. S. software; T. S. supervision; T. S. validation; T. S. visualization; T. S. writing—original draft; T. H., T. O., and M. M. writing—review and editing.

Funding and additional information—This study was supported in part by grants from the Ministry of Health, Labour, and Welfare of Japan and the Research Program on Emerging and Re-emerging Infectious Diseases program from the Japan Agency for Medical Research and Development (JP16fk0108304) to T. S. and (JP 20wm0225009) to M. M.

Conflict of interest—The authors declare that they have no conflicts of interest with the contents of this article.

Abbreviations—The abbreviations used are: 2′CM, 2′-C-methylcytidine; 2′CM-CTP, 2′-C-methylcytidine triphosphate; AS, antisense; EMSA, electrophoretic mobility shift assay; HuNV, human norovirus; IC_{50}, half of the maximal inhibitory concentration; MNV, murine norovirus; NS, nonstructural protein; PVDF, polyvinylidene fluoride; RdRp, RNA-dependent RNA polymerase; S, sense; UTR, untranslated region.

References

1. Thorne, L. G., and Goodfellow, I. G. (2014) Norovirus gene expression and replication. *J. Gen. Virol.* **95**, 278–291
2. Alhatlani, B., Vashist, S., and Goodfellow, I. (2015) Functions of the 5′ and 3′-ends of calicivirus genomes. *Virus Res.* **206**, 134–143
3. Fukushi, S., Kojima, S., Takai, R., Hoshino, F. B., Oka, T., Takeda, N., Katayama, K., and Kageyama, T. (2004) Poly(A)- and primer-independent RNA polymerase of Norovirus. *J. Virol.* **78**, 3889–3896
4. Rohayem, J., Robel, I., Jager, K., Scheffler, U., and Rudolph, W. (2006) Protein-primed and de novo initiation of RNA synthesis by norovirus 3Dpol. *J. Virol.* **80**, 7060–7069
5. Arai, H., Nishigaki, K., Nemoto, N., Suzuki, M., and Husimi, Y. (2013) Characterization of norovirus RNA replicase for *in vitro* amplification of RNA. *BMC Biotechnol.* **13**, 85
6. Subba-Reddy, C. V., Goodfellow, I., and Kao, C. C. (2011) VPg-primed RNA synthesis of norovirus RNA-dependent RNA polymerases by using a novel cell-based assay. *J. Virol.* **85**, 13027–13037
7. Jin, Z., Tucker, K., Lin, X., Kao, C. C., Shaw, K., Tan, H., Symons, J., Behera, I., Rajwanshi, V. K., Dyatkina, N., Wang, G., Beigelman, L., and

Deval, J. (2015) Biochemical evaluation of the inhibition properties of favipiravir and 2′-C-methyl-cytidine triphosphates against human and mouse norovirus RNA polymerases. *Antimicrob. Agents Chemother.* **59**, 7504–7516
8. Bull, R. A., Hyde, J., Mackenzie, J. M., Hansman, G. S., Oka, T., Takeda, N., and White, P. A. (2011) Comparison of the replication properties of murine and human calicivirus RNA-dependent RNA polymerases. *Virus Genes* **42**, 16–27
9. Rohayem, J., Jager, K., Robel, I., Scheffler, U., Temme, A., and Rudolph, W. (2006) Characterization of norovirus 3Dpol RNA-dependent RNA polymerase activity and initiation of RNA synthesis. *J. Gen. Virol.* **87**, 2621–2630
10. Simmonds, P., Karakasiliotis, I., Bailey, D., Chaudhry, Y., Evans, D. J., and Goodfellow, I. G. (2008) Bioinformatic and functional analysis of RNA secondary structure elements among different genera of human and animal caliciviruses. *Nucleic Acids Res.* **36**, 2530–2546
11. Carroll, S. S., and Olsen, D. B. (2006) Nucleoside analog inhibitors of hepatitis C virus replication. *Infect. Disord. Drug Targets* **6**, 17–29
12. Gardelli, C., Attenni, B., Donghi, M., Meppen, M., Pacini, B., Harper, S., Di Marco, A., Fiore, F., Giuliano, C., Pucci, V., Laufer, R., Gennari, N., Marcucci, I., Leone, J. F., Olsen, D. B., *et al.* (2009) Phosphoramidate prodrugs of 2′-C-methylcytidine for therapy of hepatitis C virus infection. *J. Med. Chem.* **52**, 5394–5407
13. Yunus, M. A., Lin, X., Bailey, D., Karakasiliotis, I., Chaudhry, Y., Vashist, S., Zhang, G., Thorne, L., Kao, C. C., and Goodfellow, I. (2015) The murine norovirus core subgenomic RNA promoter consists of a stable stem-loop that can direct accurate initiation of RNA synthesis. *J. Virol.* **89**, 1218–1229
14. Lin, X., Thorne, L., Jin, Z., Hammad, L. A., Li, S., Deval, J., Goodfellow, I. G., and Kao, C. C. (2015) Subgenomic promoter recognition by the norovirus RNA-dependent RNA polymerases. *Nucleic Acids Res.* **43**, 446–460
15. Filomatori, C. V., Iglesias, N. G., Villordo, S. M., Alvarez, D. E., and Gamarnik, A. V. (2011) RNA sequences and structures required for the recruitment and activity of the dengue virus polymerase. *J. Biol. Chem.* **286**, 6929–6939
16. Astier-Gin, T., Bellecave, P., Litvak, S., and Ventura, M. (2005) Template requirements and binding of hepatitis C virus NS5B polymerase during *in vitro* RNA synthesis from the 3′-end of virus minus-strand RNA. *FEBS J.* **272**, 3872–3886
17. Xiao, M., Wang, Y., Chen, J., and Li, B. (2003) Characterization of RNA-dependent RNA polymerase activity of CSFV NS5B proteins expressed in Escherichia coli. *Virus Genes* **27**, 67–74
18. D'Ambrosio, R., Degasperi, E., Colombo, M., and Aghemo, A. (2017) Direct-acting antivirals: The endgame for hepatitis C? *Curr. Opin. Virol.* **24**, 31–37
19. Prasad, B. V., Shanker, S., Muhaxhiri, Z., Deng, L., Choi, J. M., Estes, M. K., Song, Y., Palzkill, T., and Atmar, R. L. (2016) Antiviral targets of human noroviruses. *Curr. Opin. Virol.* **18**, 117–125
20. Katayama, K., Murakami, K., Sharp, T. M., Guix, S., Oka, T., Takai-Todaka, R., Nakanishi, A., Crawford, S. E., Atmar, R. L., and Estes, M. K. (2014) Plasmid-based human norovirus reverse genetics system produces reporter-tagged progeny virus containing infectious genomic RNA. *Proc. Natl. Acad. Sci. U. S. A.* **111**, E4043–E4052
21. McKenna, S. A., Kim, I., Puglisi, E. V., Lindhout, D. A., Aitken, C. E., Marshall, R. A., and Puglisi, J. D. (2007) Purification and characterization of transcribed RNAs using gel filtration chromatography. *Nat. Protoc.* **2**, 3270–3277
22. Shimoike, T., McKenna, S. A., Lindhout, D. A., and Puglisi, J. D. (2009) Translational insensitivity to potent activation of PKR by HCV IRES RNA. *Antiviral Res.* **83**, 228–237
23. Zuker, M. (1989) On finding all suboptimal foldings of an RNA molecule. *Science* **244**, 48–52
24. Chhabra, P., de Graaf, M., Parra, G. I., Chan, M. C., Green, K., Martella, V., Wang, Q., White, P. A., Katayama, K., Vennema, H., Koopmans, M. P. G., and Vinje, J. (2019) Updated classification of norovirus genogroups and genotypes. *J. Gen. Virol.* **100**, 1393–1406